**Indonesian Journal of Electrical Engineering and Informatics (IJEEI)**
Vol. 9, No. 4, December 2021, pp. 859~866
ISSN: 2089-3272, DOI: 10.52549/ijeei.v9i4.3239


# Synthesis and Characterization of $Ba_{0.6}Sr_{0.4}Fe_{12}O_{19}/LaMnO_3$ Composites as Microwave Absorbers

**Y. E. Gunanto[1], M. P. Izaak[2], H. Sitompul[3], W. A. Adi[4]**
[1,2,3] Department of Physics Education, University of Pelita Harapan, Indonesia
[4]Center for Science and Technology of Advanced Materials, BATAN, Indonesia

**Article Info**

***Article history:***

Received Jul 25, 2021
Revised Sep 25, 2021
Accepted Oct 29, 2021

***Keywords:***

Composite
hexaferrite-perovskite
absorber
microwave
hard-soft magnetic

**ABSTRACT**

The synthesis and characterization of $Ba_{0.6}Sr_{0.4}Fe_{12}O_{19}/LaMnO_3$ composite material has been successfully carried out by mechanical alloying method using high energy milling. Crystal structure and surface morphology were characterized using x-ray diffraction and scanning electron microscopy. While the value of magnetization and the ability to absorb microwaves, vibrating sample magnetization and vector network analyzing were used, respectively. With variations in weight, does not change the crystal structure. The $Ba_{0.6}Sr_{0.4}Fe_{12}O_{19}$ phase has a hexagonal structure and the $LaMnO_3$ phase has an orthorhombic structure. Surface morphology has a heterogeneous size in the range of 200-450 nm with the form of platelets. The best composite material $Ba_{0.6}Sr_{0.4}Fe_{12}O_{19}/LaMnO_3$ (75/25 wt%) is with composition of 75/25 wt%, and has magnetic properties with a magnetic saturation of Ms ~ 46.83 emu/g, Mr ~ 28.8 emu/g, and a coercive field of Hc ~ 3.88 kOe. The minimum reflection loss value is – 13.0 dB at 11.2 GHz frequency and broadband absorber with RL of -8dB at 8-12 GHz.



***Corresponding Author:***

Y. E. Gunanto,
Department of Physics Education,
University of Pelita Harapan,
Karawaci, Tangerang 15811, Indonesia.
Email: yohanes.gunanto@uph.edu

## 1. INTRODUCTION

Hexaferrite-based materials, especially M-type hexaferrite ($MFe_{12}O_{19}$, M = Ba or Sr) are still a concern of researchers [1-3]. At room temperature type-M hexaferrite material is hard magnetic, has high magnetic saturation Ms, wide Hc coercivity field, strong uniaxial magnetic anisotropy, high curie temperature, and good chemical stability. Therefore, this material is very applicable in technology, for example as a recording medium [1], ceramic color pigments [2], photocatalysts [3], and microwave absorbers at a frequency of 8-12 GHz [4].

A good material as an absorber of electromagnetic waves must have high permeability and permittivity [5]. So the material is in a hard-soft magnetic state. Therefore, to increase the capability of M-type hexaferrite material as a microwave absorber, several methods were carried out, for example combining $Ba^{2+}$ and $Sr^{2+}$ ions ($Ba_{1-x}Sr_xFe_{12}O_{19}$) [6], substituting $Mn^{2+}$ ions on $Fe^{3+}$ ions ($Ba_{0.6}Sr_{0.4}Fe_{12-z}Mn_zO_{19}$) [4], making hexaferrite composites with perovskite ($SrFe_{12}O_{19}$–$La_{1-x}Sr_xMnO_3$) [7], $BaFe_{12}O_{19}$-$NiFe_2O_4$ composites [8], or making multiple layers consisting of $BaFe_{12}O_{19}$-$BaCoZnFe_{10}O_{19}$ composites [9].

Several sampling methods that have been used so far are co-precipitation [1, 8], Salt Flux-Assisted [2], auto-combustion [7], mechanical alloying using milling [4,10]. Mechanical alloying method is the easiest and cheapest method.

From the previous study, the substitution of $Mn^{2+}$ ions on $Fe^{3+}$ ions ($Ba_{0.6}Sr_{0.4}Fe_{12}$-$zMnzO_{19}$) with z = 0, 1, 2, and 3. They reported that for z = 0 ($Ba_{0.6}Sr_{0.4}Fe_{12}O_{19}$) the magnetic properties were Ms = 92.9 emu/g and Hc = 0.424 T, while a maximum reflection loss (RL) of about -4.9 dB in a frequency range of 12.5 GHz

and RL of -2 dB in a frequency range of 8-10 GHz for a sample thickness of 1.5 mm [4]. In other research for $La_{1-x}Ba_xMnO_3$ perovskite sample with a sample thickness of 1.5 mm has a value of RL ~ - 2.6 dB at a frequency of 11 GHz [11] with a magnetic saturation value of Ms ~ 9 emu/g and Hc ~ 90 Oe [12]. Meanwhile, the $La_{1-x}Ca_xMnO_3$ perovskite sample for x = 0.1 has Rl ~ - 42 dB (f = 10.5 GHz) for a sample thickness of 2.0 mm [13]. Based on the results of previous studies, it was stated that $Ba/SrFe_{12}O_{19}$ material has low reflection loss but the absorption frequency area is relatively wide, while $LaMnO_3$ material has high reflection loss but relatively narrow absorption. Thus, in this study, a combination of the two materials was carried out to form a composite in the hope of obtaining a material that has a high reflection loss with a relatively wide absorption frequency area. So the purpose of this research is to synthesize and characterize the superior material in the form of $Ba_{0.6}Sr_{0.4}Fe_{12}O_{19}/LaMnO_3$ composite as a microwave absorbing material at a frequency of 8-12 GHz using mechanical milling method. This research is an initial study on the development of composite materials which can then be used as a reference for the modification of the two materials so that a more optimal microwave absorbing material can be obtained.

## 2. RESEARCH METHOD

### 2.1. Precursor Preparation

Raw materials consisting of $BaCO_3$, $SrCO_3$, and $Fe_2O_3$, each Merck product with purity > 99% were mixed by stoichiometric calculations to form the sample composition $Ba_{0.6}Sr_{0.4}Fe_{12}O_{19}$.
The equations used are as follows:

$$0.6\ BaCO_3 + 0.4\ SrCO_3 + 6\ Fe_2O_3 \rightarrow Ba_{0.6}Sr_{0.4}Fe_{12}O_{19} + CO_2 \quad (1)$$

For samples, $LaMnO_3$ was made from materials $La_2O_3$ (Aldrich, 99%) and $MnCO_3$ (Merck, 99%) with equation (2):

$$La_2O_3 + 2\ MnCO_3 \rightarrow 2\ LaMnO_{3-\partial} + 2\ CO_2 \quad (2)$$

The $Ba_{0.6}Sr_{0.4}Fe_{12}O_{19}/LaMnO_{3-\partial}$ composite was made with three different compositions, each with a weight % ratio of 85/15, 75/25, and 65/35. Each composite composition was mixed in a stainless steel vial, given iron balls with a ratio of iron:sample weight = 1:1 and added ethanol up to two-thirds. Each sample was milled for 30 hours using high energy milling at 700 rpm with a mechanism of every hour milling, interspersed with 0.5 hours of rest. This is to avoid the heat that occurs due to the impact of the iron balls with the vial. Then the sample was sintered at 1000 ºC for 5 hours under atmospheric pressure.

### 2.2. Characterization

X-ray diffractometer (XRD) type PAN Analytical Empyrean ($\lambda$Cu-Kα, = 1.5406 Å) was used to characterize the phase formation and the composition formed. Data analysis of XRD results both qualitatively and quantitatively using Rietvelt software. The surface morphology was characterized using a scanning electron microscopy (SEM) type-JEOL JED 2300. Meanwhile, the characterization of magnetic magnitude at room temperature and the ability to absorb microwaves were characterized by vibrating-sample magnetometer (VSM) OXFORD VSM 1.2H and Vector Network, respectively. Analysis (VNA) type-Anritsu MS46322A in the 8-12 GHz frequency range.

## 3. RESULTS AND DISCUSSION

The $Ba_{0.6}Sr_{0.4}Fe_{12}O_{19}/LaMnO_3$ composite with a weight ratio of 85/15 wt%, 75/25 wt%, and 65/35 wt% will be referred to as YEG-1, YEG-2, and YEG-3, respectively. Figure 1 shows the results of X-ray diffraction characterization for samples YEG-1, YEG-2, and YEG-3. All samples showed typical peaks of their constituent materials, namely the phases of $Ba_{0.6}Sr_{0.4}Fe_{12}O_{19}$ (JCPDS card no. 00-051-1879) and $LaMnO_3$ (JCPDS Card No. 54-1275). See Figure 1(a). Figures 1 (b)-(d) show the results of refining the diffraction pattern using the Rietvelt program. The complete refinement results using the Rietvelt program can be seen in Table 1. In the three samples, the fase $Ba_{0.6}Sr_{0.4}Fe_{12}O_{19}$ phase has a hexagonal crystal structure, the P63/mmc space group and the $LaMnO_3$ phase has an orthorhombic crystal structure, the Pbnm space group. The same result was also obtained in our previous study, where $Ba_{0.6}Sr_{0.4}Fe_{12-3x}Zn_{2x}Ti_xO_{19}$ for x = 0 had a hexagonal crystal structure [14]. Different results were obtained for the $LaMnO_3$ sample, where the crystal structure was hexagonal [15]. According to A. Gholizadeh, $LaMnO_3$ can have an orthorhombic, rhombohedral or cubic structure, depending on the concentration of $Mn^{4+}$ ions [12]. If the $Mn^{4+}$ ion content is around 0-12%, it has an orthorhombic structure. In this paper, the Mn ion is in the $Mn^{2+}$ ($MnCO_3$) state which then becomes $Mn^{3+}$ ($LaMnO_3$). Thus the state of the $Mn^{4+}$ ion does not exist. From Table 1. it can be seen that as the percentage by weight of $LaMnO_3$ decreases (the percentage by weight of $Ba_{0.6}Sr_{0.4}Fe_{12}O_{19}$ decreases), the crystal density of the $Ba_{0.6}Sr_{0.4}Fe_{12}O_{19}$ phase also decreases, although it is relatively not large. The composition ratio by weight of $Ba_{0.6}Sr_{0.4}Fe_{12}O_{19}$-$LaMnO_3$ formed was 86%-14%, 74%-26%, and 63%-37%, respectively.

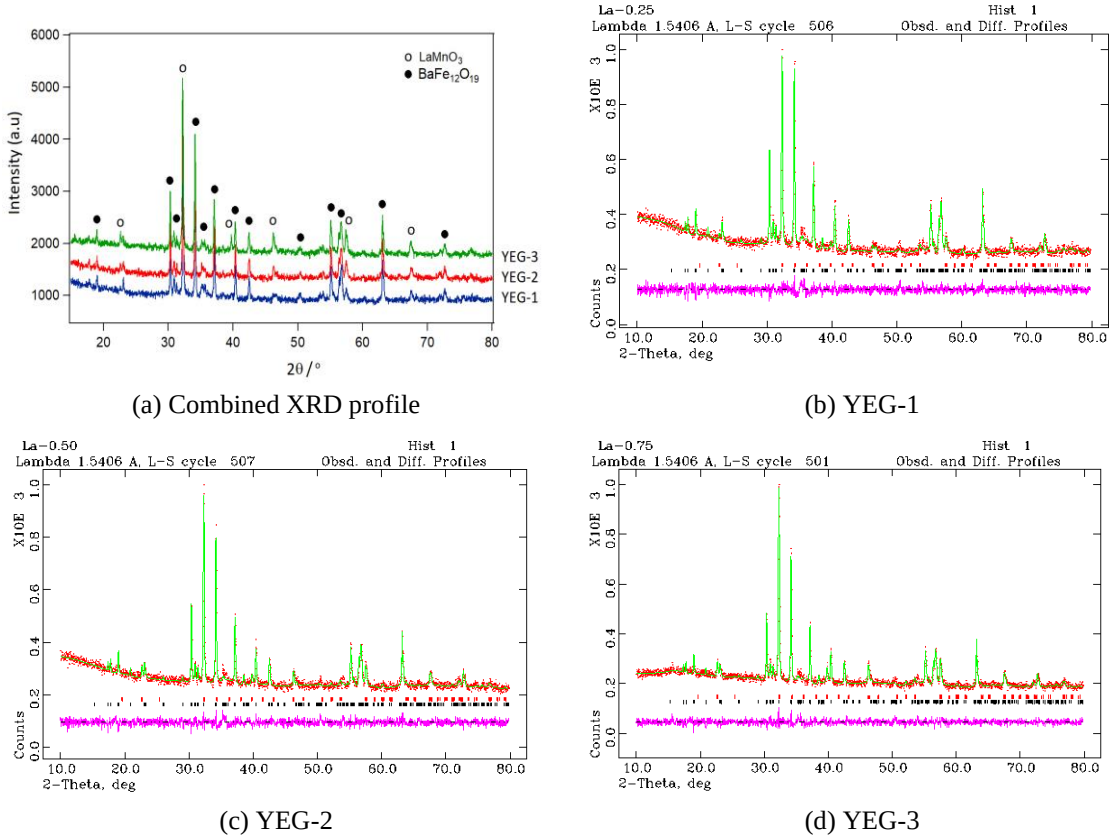


(a) Combined XRD profile (b) YEG-1

(c) YEG-2 (d) YEG-3

Figure 1. (a) X-ray diffraction pattern for samples YEG-1, YEG-2, and YEG-3. (b)-(d) Refine results using the Rietvelt program for samples YEG-1, YEG-2, and YEG-3, respectively.

The results of the analysis of the three samples have met the criteria of the Rietveld method with a value of $\chi^2$ close to 1. This means that the sintering process of the mixture does not affect the phase change of the two composite-forming materials. However, it is hoped that with this sintering process, there will be intergrain interactions between $Ba_{0.6}Sr_{0.4}Fe_{12}O_{19}$ and $LaMnO_3$ materials. This condition is very necessary for microwave absorbing materials because the microwave absorption mechanism is strongly influenced by the magnetic and electrical properties of the material [5]. Table 1 shows that the volume of the YEG-1, YEG-2, and YEG-3 composite V unit cells for the $BaFe_{12}O_{19}$ phase ranges from 693.4 to 693.6 Å$^3$ with atomic density ranging from 5.874-5.876 g/cm3, while for the $LaMnO_3$ phase it ranges from 240.7 to 240.9 Å$^3$. with atomic densities ranging from 6.666 to 6.673 g/cm$^3$. This means that these two materials do not undergo structural changes after being composited through the sintering process.

Table 1. Resume of diffraction pattern analysis results using the Rietvelt program.

| Sample | Phase | System | SG | Lattice parameters (Å) | | | V | ρ | $\chi^2$ | fraction |
|---|---|---|---|---|---|---|---|---|---|---|
| | | | | *a* | *b* | *c* | (Å$^3$) | (g/cm$^3$) | | % |
| YEG-1 | $BaFe_{12}O_{19}$ | Hexagonal | P63/mmc | 5.8851(3) | 5.8851(3) | 23.118(2) | 693.4(1) | 5.876 | 1.036 | 85.93 |
| | $LaMnO_3$ | Orthorombic | Pbnm | 5.545(5) | 5.555(6) | 7.815(5) | 240.7(3) | 6.673 | | 14.07 |
| YEG-2 | $BaFe_{12}O_{19}$ | Hexagonal | P63/mmc | 5.8852(3) | 5.8852(3) | 23.122(2) | 693.5(1) | 5.875 | 1.036 | 73.86 |
| | $LaMnO_3$ | Orthorombic | Pbnm | 5.550(2) | 5.531(3) | 7.847(4) | 240.9(1) | 6.666 | | 26.14 |
| YEG-3 | $BaFe_{12}O_{19}$ | Hexagonal | P63/mmc | 5.8853(2) | 5.8853(2) | 23.123(2) | 693.6(1) | 5.874 | 1.032 | 63.31 |
| | $LaMnO_3$ | Orthorombic | Pbnm | 5.551(6) | 5.545(7) | 7.825(2) | 240.9(1) | 6.667 | | 36.69 |

The results of the XRD analysis are also supported based on observations of the microstructure of this composite which is expected to produce a homogeneous mixture and have a relatively uniform particle size as shown in Figure 2. Figure 2 (a)-(c) shows a scanning electron microscopy (SEM) image of the microstructure of the $Ba_{0.6}Sr_{0.4}Fe_{12}O_{19}$ composite with perovskite $LaMnO_3$ with various weight percentage fractions of 85/15, 75/25, and 65/35. The granules form like platelets, as seen in the insert in Figure 2 (c). The grain size ranges from 200 to 450 nm. This measure is obtained by comparing the grain length to the existing scale. $Ba_{0.6}Sr_{0.4}Fe_{12}O_{19}$ phase and $LaMnO_3$ phase were mixed evenly. However, we suspect that based on the crystal size results, the small grains represent the $LaMnO_3$ phase, while the larger grains represent the $Ba_{0.6}Sr_{0.4}Fe_{12}O_{19}$ phase. Similar results were also obtained by J. N. Dahal et al., where the hexaferrite particle size was larger than the perovskite particle size [7]. The size of the particles formed is also influenced by the sintering temperature. The higher the temperature, the larger the particle size that's formed [16].

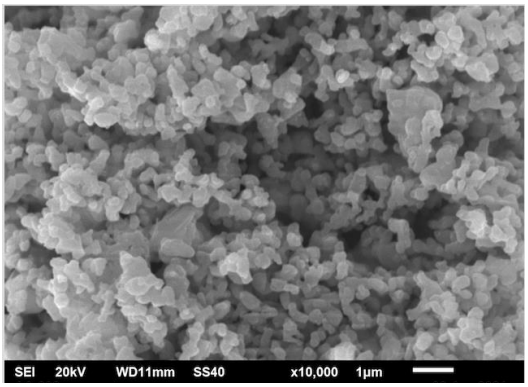


(a) YEG-1

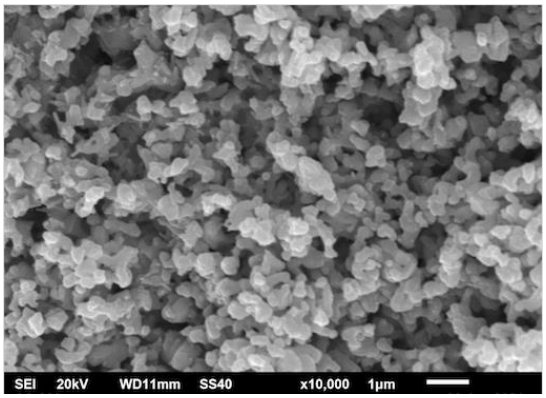


(b) YEG-2

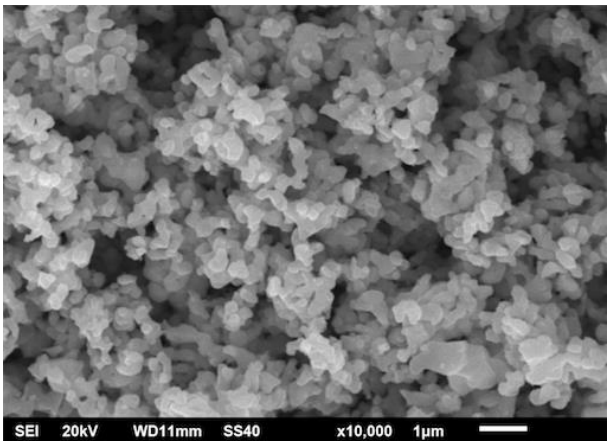


(c) YEG-3

Figure 2. Surface morphology of SEM results for samples (a) YEG-1, (b) YEG-2, and (c) YEG-3.

From the observation of the microstructure, it is shown that these three composites are homogeneous mixtures with relatively uniform particle sizes. This means that the distribution of particles in the mixture between $BaFe_{12}O_{19}$ and $LaMnO_3$ is evenly distributed over the entire sample surface in these three composites. Besides that, it also appears that the particles are not dispersed but there is good interconnection between the particles so that intergrain interactions are expected between the $BaFe_{12}O_{19}$ and $LaMnO_3$ materials. The presence of this intergrain interaction will greatly affect the magnetic properties and microwave absorption characteristics of the composite, especially in composites consisting of a mixture of materials that have much different characteristics [17]. $BaFe_{12}O_{19}$ material is a ferrous magnetic material that has hard magnetic characteristics with relatively large magnetic properties so that it tends to have a relatively large permeability value, while $LaMnO_3$ material is an antiferrous magnetic material but has a relatively high permittivity value.

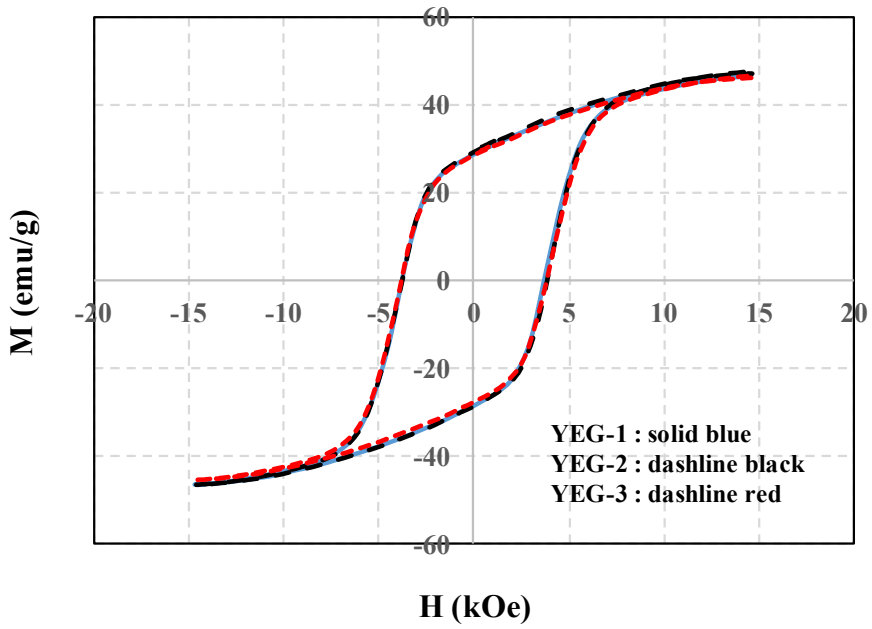


Figure 3. Magnetic hysteresis loop curves of YEG-1, YEG-2, and YEG-3 samples at room temperature.

Magnetic hysteresis loop curves at room temperature for YEG-1, YEG-2 and YEG-3 composites are shown in Figure 3. The three samples have remanent magnetic magnitude Mr and coercivity field Hc are relatively the same, but differ in magnetic saturation values Ms. Compared to the other two samples, YEG-2 sample has the highest Ms saturation magnetic value, around 46.83 emu/g. The complete results of VSM can be seen in Table 2. At room temperature $Ba_{0.6}Sr_{0.4}Fe_{12}O_{19}$ is hard magnetic, has a magnetic saturation of Ms of 92.9 emu/g and a coercive field of Hc = 4.24 kOe [4, 14], and $LaMnO_3$ has a value of Ms ~ 3.42 emu/g and Hc ~ 0.755 kOe are soft magnetic [7, 18, 19]. The $Ba_{0.6}Sr_{0.4}Fe_{12}O_{19}$-$LaMnO_3$ composite is a hard-soft magnetic. The magnitude of the magnetization can be seen in Table 2.

Table 2. Magnetization of Ms, Mr and Hc at room temperature

| Sample | Ms (emu/g) | Mr (emu/g) | Hc (kOe) |
|---|---|---|---|
| YEG-1 | 46.17 | 28.80 | 3.88 |
| YEG-2 | 46.83 | 28.80 | 3.88 |
| YEG-3 | 46.83 | 28.80 | 3.88 |

Based on the measurement results in Table 2, it appears that the magnetic properties of this material are relatively unchanged, this indicates that the level of particle homogeneity and the effect of the presence of intergrain interactions in the particles plays an important role in maintaining the magnetic properties of this composite. It is also suspected that this $LaMnO_3$ system when interacting with $Ba^{2+}$ ions will be ferromagneticly so that it is able to maintain the Ms of this composite even though the $BaFe_{12}O_{19}$ fraction is decreasing [20]. It is different if this composite is purely mixed without any sintering process, in general the saturation magnetization of Ms tends to decrease due to the reduced mass fraction of the $BaFe_{12}O_{19}$ phase in the composite. These results are in agreement with the results of the previous analysis using XRD and microstructure observations using SEM. This study can also be seen from the measurement results of microwave absorption, as the main goal of this research.

The ability of a material to absorb electromagnetic waves is usually referred to as the reflection loss of electromagnetic radiation, RL (dB), calculated by the following equation: [21-22]

$$RL(dB)= 20 \log|(Z_{in} - Z_0 )/(Z_{in}+Z_0 |) \quad (3)$$

where $Z_{in}$ and $Z_0$ represent the characteristic impedance of the material and the characteristic impedance of vacuum, respectively. The Zin value is obtained from the equation:

$$Z\_in= (\mu_r/\varepsilon_r )^{(1/2)} \tanh[j(2\pi fd/c) (\mu_r \varepsilon_r )^{(1/2)} ] \quad (4)$$

where $\mu_r$ and $\varepsilon_r$ are the relative permeability and permittivity of the material, d is the thickness of the sample, c is the speed of electromagnetic waves in a vacuum, and f is the frequency with which the waves arrive. According to equation (3), when RL = - 10 dB, the wave absorption reaches 90%.

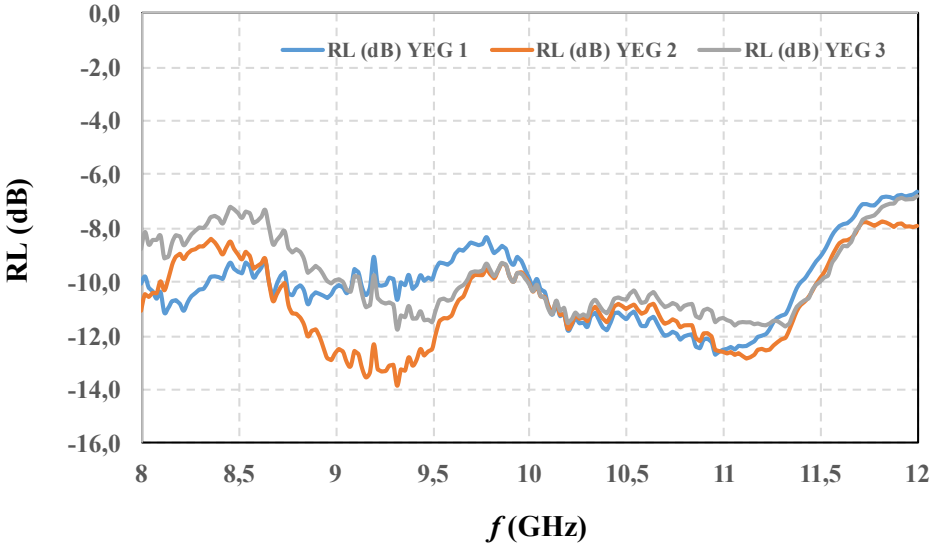


Figure 4. Frequency dependent reflection loss (RL) for YEG-1, YEG-2, and YEG-3 samples.

The reflection loss for the YEG-1, YEG-2, and YEG-3 samples can be seen in Figure 4. The best minimum reflection loss is obtained for the YEG-2 sample, which is – 13.0 dB, f = 11.12 GHz, and 1.52 GHz bandwidth. The increase in the weight percentage of $LaMnO_3$ in the $Ba_{0.6}Sr_{0.4}Fe_{12}O_{19}$-$LaMnO_3$ composite, although only slightly, the bandwidth increased from 1.42 GHz to 1.52 GHz, there was also a shift in the peak frequency from 10.96 GHz to 11.22 GHz. The amount of reflection loss (RL) by the absorbing material is influenced by electromagnetic parameters, such as permittivity and permeability of the material. Therefore, the soft magnetic properties of $LaMnO_3$ strengthen the microwave attenuation performance in the high frequency region [20]. While $Ba_{0.6}Sr_{0.4}Fe_{12}O_{19}$ is a hard magnetic having a high Ms, so it will widen the absorption band [23].

Table 3. Value of reflection loss (RL), frequency and bandwidth for YEG-1, YEG-2, dan YEG-3 samples

| Sample | RL max (dB) | *f* (GHz) | RL (dB) | Freq. range (GHz) |
|---|---|---|---|---|
| YEG-1 | | | -6.92 | 8.0-12.0 (4.0) |
| | -11.21 | 8.12 | -10.00 | 8.0-8.36 (0.36) |
| | -10.62 | 8.96 | -10.19 | 8.64-9.44 (0.8) |
| | -12.71 | 10.96 | -11.62 | 10.0-11.42 (1.42) |
| YEG-2 | | | -8.0 | 8.0-12.0 (4.0) |
| | -10.61 | 8.04 | -10.30 | 8.0-8.14 (0.14) |
| | -13.91 | 9.32 | -10.10 | 8.64-9.70 (1.06) |
| | -13.02 | 11.12 | -10.04 | 9.98-11.50 (1.52) |
| YEG-3 | | | -6.81 | 8.0-12.0 (4.0) |
| | -11.52 | 9.50 | -10.11 | 9.04-9.68 (0.64) |
| | -11.61 | 11.22 | -10.10 | 9.98-11.50 (1.52) |

In Table 3, it can be seen that the performance improvement of this composite-based microwave absorbing material is obtained, namely reflection loss and the width of the microwave absorption area. It is known that before being modified these two materials have low reflection loss, but when they become composites and it is strongly suspected that interconnection occurs between grains, this results in the composite having higher permeability and permittivity so as to produce higher microwave absorption. The most

interesting thing is that the absorption frequency area becomes wider. The YEG-2 composite found microwave absorption with RL = -8 dB at a wide frequency from 8-12 GHz. This composition becomes a reference and initial study for the development of further composite materials, so that it is expected that composite materials with more optimum absorption capabilities can be obtained.

## 4. CONCLUSION

The $Ba_{0.6}Sr_{0.4}Fe_{12}O_{19}/LaMnO_3$ composite material which has been successfully synthesized by mechanical alloying method has a hexagonal/orthorhombic crystal structure with a homogeneous mixture and relatively uniform particle size of about 200 to 450 nm. This sintering process produces interconnections between particles in the composite so that it is suspected. Intergrain interactions occur which are able to maintain their magnetic properties even though the $BaFe_{12}O_{19}$ fraction is reduced. Besides that, it produces a significant increase in microwave absorption capability with a relatively wide absorption frequency area of 8-12 GHz with a reflection loss of -8 dB. This research can be used as a reference and initial study for the development of further composite materials in order to obtain composite materials with more optimum absorption capabilities.

## ACKNOWLEDGMENTS

The funding for this research was supported by Pelita Harapan University, through the research contract number: 075/LPPM-UPH/II/2021 and The Menristek-Dikti through a Higher Education Basic Research Contract for the 2021 Budget Year with the contract number: 297/LPPM-UPH/IV/2021, in accordance with the Research Grant Implementation Assignment Agreement Letter Number: 1218/LL3/PG/2021, April 1, 2021 through the Primary Research Scheme for Higher Education Fiscal Year 2021.

## REFERENCES

[1] M. ME. Barakat , D. E. -S. Bakeer, and A. –H. Sakr, "Structural, Magnetic Properties and Electron Paramagnetic Resonance for $BaFe_{12-x}Hg_xO_{19}$ Hexaferrite Nanoparticles Prepared by Co- Precipitation Method," *Journal of Taibah University for Science*., vol.14, no.1, pp. 640-652, 2020.

[2] B. C. Brightlin, and S. Balamurugan, "Magnetic, Micro-structural, and Optical Properties of Hexaferrite, $BaFe_{12}O_{19}$ Materials Synthesized by Salt Flux-Assisted Method," *J. Supercond Nov Magn*., vol.29, no.9, 2016.

[3] Z. H. Karahroudi, K. Hedayati, and M. Goodarzi, "Green synthesis and characterization of hexaferrite strontium-perovskite strontium photocatalyst nanocomposites," *De Gruyter, Main Group Met. Chem*., vol. 43, no.1, pp. 26–42, 2020.

[4] Y. E. Gunanto, E. Jobiliong, and W. A. Adi, "Microwave Absorbing Properties of $Ba_{0.6}Sr_{0.4}Fe_{12-z}Mn_zO_{19}$ (z = 0 – 3) Materials in X-Band Frequencies," *J. Math. Fund. Sci.*, vol. 48, no. 1, pp. 55-65, 2016.

[5] W. A. Adi, Yunasfi, Mashadi, D. S. Winatapura, A.Mulyawan, Y. Sarwanto, Y. E. Gunanto and Y. Taryana, *Electromagnetic Fields and Waves*, IntechOpen, 2019.

[6] Y. Marouani, J. Massoudi, M. Noumi, A. Benali, E. Dhahri, P. Sanguino, M. P. F. Graça, M. A. Valente, and B. F. O. Costa, "Electrical conductivity and dielectric properties of Sr doped M-type barium *hexaferrite* $BaFe_{12}O_{19}$*," RSC Adv.*, vol.11, pp.1531–1542, 2021.

[7] J. N. Dahal, D. Neupane, and T. P. Poudel, "Synthesis and magnetic properties of 4:1 hard-soft $SrFe_{12}O_{19}$–$La_{1-x}Sr_xMnO_3$ nanocomposite prepared by auto-combustion method," *AIP Advances*., vol.9, no.075308, 2019.

[8] C. Thirupathy, S. C. Lims, S. J. Sundaram, A. H. Mahmoud, and K. Kaviyarasu, "Equilibrium synthesis and magnetic properties of $BaFe_{12}O_{19}/NiFe_2O_4$ nanocomposite prepared by co precipitation method," *Journal of King Saud University – Science*., vol. 32, pp. 1612–1618, 2020.

[9] E. Handoko, S. Budi, I. Sugihartono, M. A. Marpaung, Z. Jalil, A. Taufiq, and M. Alaydrus, "Microwave absorption performance of barium hexaferrite multi-nanolayers," *Mater. Express.*, vol. 10, no. 8, 2020.

[10] Y. E. Gunanto, E. Jobiliong, and W. A. Adi, "Composition and Phase Analysis of Nanocrystalline $Ba_xSr_{1-x}Fe_{12}O_{19}$ (x = 1.0; 0.6; and 0.4) by Using General Structure Analysis System," *AIP Conference Proceedings*., vol.1719, no. 030019, 2016.

[11] P. Sardjono P, WA. Adi Structural, Magnetic and Electrical Properties of $La_{1-x}Ba_xMnO_3$ for Absorber Electromagnetic Wave. J. Basic. Appl. Sci. Res. ;3: 230-234, 2013.

[12] A.Gholizadeh, "X-Ray Peak Broadening Analysis in $LaMnO_{3+\delta}$ Nano-Particles with Rhombohedral Crystal Structure," *Journal of Advanced Materials and Processing*, vol.3, no.3, pp. 71-83, 2015.

[13] J. W. Liu, J. Wang, and H. T. Gao, "Infrared Emissivities and Microwave Absorption Properties of Perovskite $La_{1-x}Ca_xMnO_3$ ($0 \le x \le 0.5$)," *Materials Science Forum*., vol.914, pp. 96-101, 2018.

[14] Y. E. Gunanto, Y. Sarwanto, and W. A. Adi, "Analysis of Crystallography Structure and Magnetic Properties of Microwave Absorbing Material $Ba_{0.6}Sr_{0.4}Fe_{12-3x}Zn_{2x}Ti_xO_{19}$ (x = 0, 0.2, 0.4, and 0.6)," *Key Engineering Materials*., vol. 855, pp 293-298, 2020.

[15] E. Hernández, V. Sagredo, and G.E. Delgado, "Synthesis and magnetic characterization of $LaMnO_3$ nanoparticles," *Revista Mexicana de Física*., vol.61, pp.166–169. 2015.

[16] E. Roohani, H. Arabi, R. Sarhaddi, S. Sudkhah, and A. Shabani, "Effect of annealing temperature on structural and magnetic properties of strontium hexaferrite nanoparticles synthesized by sol-gel auto-combustion method," *International Journal of Modern Physics B.*, vol. 29, no. 1550190, 2015.
[17] W.A. Adi, Yunasfi. Magnetic properties and microwave absorption characteristic of MWNT filled with magnetite coated iron nanoparticles. Materials Science and Engineering: B; 262: 114760, 2020.
[18] T. H. Tran, T. H. Phi, H. N. Nguyen, N. H. Pham, C. V. Nguyen, K. H. Ho, Q. K. Doan, V. Q. Le, T. T. Nguyen, and V.T. Nguyen, "Sr doped $LaMnO_3$ nanoparticles prepared by microwave combustion method: A recyclable visible light photocatalyst," *Results in Physics*., vol.19. no.103417, 2020.
[19] W. A. Adi, A. Manaf, and Ridwan. Absorption characteristics of the electromagnetic wave and magnetic properties of the $La_{0.8}Ba_{0.2}Fe_xMn_{1/2(1-x)}Ti_{1/2(1-x)}O_3$ (x = 0.1-0.8) perovskite system. International Journal of Technology; 8: 887-897, 2017.
[20] E. Sukirman, Y. Sarwanto, W. A Adi, A. Insani A, and F. Buys. Weak Ferromagnetic Property and Electromagnetic Waves Absorption Characteristic of $La_{(1-x)}Ba_xMnO_3$. International Journal of Engineering Materials and Manufacture; 4: 96-106, 2019.
[21] G. Kulkarni, P. Kandesar, N. Velhal, H. Kim, and V. Puri, "Facile synthesis of coral cauliflower-like polypyrrole hemispheres toward screening electromagnetic interference pollution," *J Appl Polym Sci*., 2021.
[22] Yunasfi, A. Mulyawan, Mashadi, D S. Winatapura, and W. A. Adi. Magnetic and microwave absorption properties of $La^{3+}$-substituted manganese ferrites synthesized via solid-state reaction method. Applied Physics A, 127:763, 2021; https://doi.org/10.1007/s00339-021-04907-w
[23] Zhao, J. et al. "$BaFe_{12}O_{19}$-chitosan Schi -base Ag (I) complexes embedded in carbon nanotube networks for high-performance electromagnetic material," *Sci. Rep*. vol.5, no.12544, 2015.